NANO LETTERS

LETTER

pubs.acs.org/NanoLett

Superplastic Deformation of Defect-Free Au Nanowires via Coherent Twin Propagation

Jong-Hyun Seo,[†,‡,▽] Youngdong Yoo,[§,▽] Na-Young Park,[∥] Sang-Won Yoon,[†,‡] Hyoban Lee,[§] Sol Han,[§] Seok-Woo Lee,[⊥] Tae-Yeon Seong,[‡] Seung-Cheol Lee,[¶] Kon-Bae Lee,[∥] Pil-Ryung Cha,[∥] Harold S. Park,[#] Bongsoo Kim,[*,§] and Jae-Pyoung Ahn[*,†]

[†]Nano Analysis Center, KIST, Seoul 130-650, Korea

[‡]Advanced Material Division, Korea University, Seoul 136-701, Korea

[§]Department of Chemistry, KAIST, Daejeon 305-701, Korea

[∥]School of Advanced Materials Engineering, Kookmin University, Seoul 136-702, Korea

[⊥]Department of Materials Science and Engineering, Stanford University, Stanford, California 94305-2205, United States

[¶]Computational Science Center, KIST, Seoul 130-650, Korea

[#]Department of Mechanical Engineering, Boston University, Boston, Massachusetts 02215, United States

Supporting Information

ABSTRACT: We report that defect-free Au nanowires show superplasticity on tensile deformation. Evidences from high-resolution electron microscopes indicated that the plastic deformation proceeds layer-by-layer in an atomically coherent fashion to a long distance. Furthermore, the stress−strain curve provides full interpretation of the deformation. After initial superelastic deformation, the nanowire shows superplastic deformation induced by coherent twin propagation, completely reorientating the crystal from <110> to <100>. Uniquely well-disciplined and long-propagating atomic movements deduced here are ascribed to the superb crystallinity as well as the radial confinement of the Au nanowires.

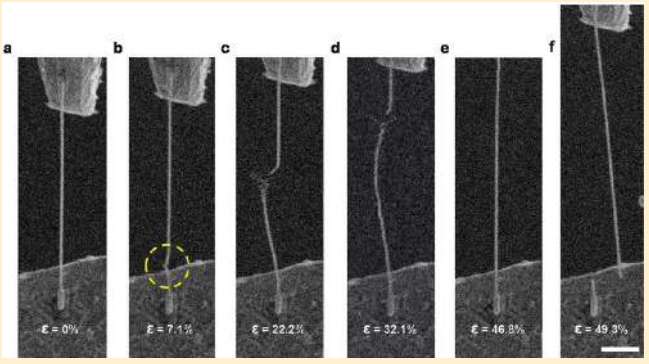

KEYWORDS: gold, nanowire, mechanical, superplastic, tensile, deformation

How would individual atoms in material actually move under mechanical force? In crystalline materials, microscopic atomic movements over one another during a mechanical process are inherently related with macroscopic mechanical properties.[1−4] To decipher the deformation mechanism on an atomic scale, however, defect-induced complex interactions that would seriously puzzle the whole mechanical process should be greatly reduced.[4−8] Fabricating defect-free material can be possible by reducing its size below a certain critical value.[9] Defect-free metal nanowires (NWs) are ideal model systems to explore tensile properties at the nanoscale, since they are free of complex interactions and have well-defined geometries and high aspect ratios.[10] While atomistic simulations have interestingly predicted strong but ductile behavior of single-crystalline metal NWs through deformation twinning,[11−13] only a few experimental studies have been reported on tensile processes of metal NWs,[14−16] of which the plastic deformation has not been observed yet. The successful tensile experiment should meet highly stringent requirements including preparation of samples of extreme crystallinity, delicate manipulation, and an exact alignment of the NW along the tensile force.

We synthesized defect-free single-crystalline Au NWs via vapor transport method[10] and investigated their tensile deformation. Through in situ scanning electron microscope (SEM) and high-resolution transmission electron microscope (HRTEM), we observed a unique deformation behavior that begins with superelastic deformation followed by large scale plastic deformation. We found that the plastic deformation proceeds by the formation and propagation of twins, in which the Au atoms move coherently in a group. Furthermore, we acquired a stress−strain curve for the entire tensile deformation process that provides crucial information on principal mechanical properties. From the combined information obtained by in situ SEM, HRTEM, and the stress−strain curve, we intend to explore the tensile deformation of Au NWs in an atomic detail and pursue to find insights on the general mechanical deformation process.

The Au NWs were synthesized by a vapor-transport method on a sapphire (0001) substrate as previously described by Yoo et al.[10] and had atomically smooth surfaces, diameters of 40−150 nm,

Received: July 1, 2011
Published: July 14, 2011

dx.doi.org/10.1021/nl2022306 | *Nano Lett.* 2011, 11, 3499–3502

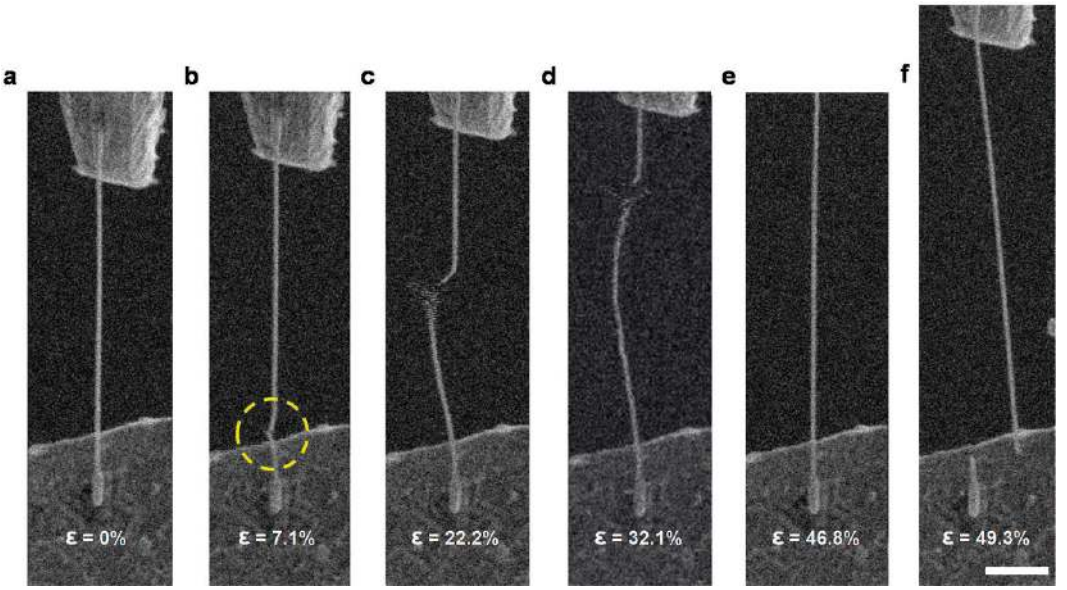

Figure 1. Snapshots on the tensile deformation of a ⟨110⟩ Au NW. (a−f) SEM images captured from Supporting Information Movie S1 that shows the entire tensile process until a final fracture of a Au NW. ε represents total strain in each tensile stage. A yellow circle in (b) highlights an arch-shaped feature formed at an initial stage of plastic deformation. The scale bar is 1 μm.

lengths of 5−20 μm, a rhombic cross-section with four equivalent {111} side facets, and ⟨110⟩ growth direction (Supporting Information Figure S1). Repeated transmission electron microscopy (TEM) investigations confirmed that the NWs are single-crystalline and defect-free.

Tensile experiments were performed using a nanomanipulator (MM3A, Kleindeck) installed in a FIB system (Quanta 3D, FEI). For the tensile test, one end of a Au NW was first attached to a tungsten tip on the nanomanipulator using e-beam assisted Pt deposition. The other end of a Au NW was then welded onto a TEM half grid (GRD-0001.01.01, Omniprobe) using e-beam assisted Pt deposition for TEM observations. The experimental configuration of a tungsten tip, NW, and Cu grid is perpendicular to the direction of e-beam in order to observe a whole process during the tensile test (Supporting Information Figure S2). The NW is subsequently pulled in tension at a rate of 1.9×10^{-7} m/sec. The deformation behavior of Au NWs was observed using a TEM (Titan80-300, FEI) at an each deformation stage. For the tensile measurements, the flow stress is calculated by dividing load (N) by area (nm^2). The load is obtained by the force measurement system attached onto a cantilever and the cross-sectional area of a Au NW is measured by TEM. The entire tensile process of the Au NW is illustrated by a series of SEM images in Figure 1 and a video (Supporting Information Movie S1). The NW has a diameter of 88 ± 10 nm. Initially, a small arch-shaped feature appeared near the bottom of the Au NW (Figure 1b). The feature expanded gradually along the tensile direction (Figure 1d) until the final fracture near the bottom with a total strain of 50% (Figure 1f).

More detailed information is acquired from a series of TEM images of the NW obtained during the whole deformation process by stopping the tensile load at critical steps, cutting the NW using the FIB and then taking TEM snapshots (Supporting Information Figure S3). The TEM images in Figure 2 illustrate how the atomic crystal structure of the arch-shaped extension in Figure 1 changes during the tensile loading process. Figure 2a,b displays two nanoscale twin nuclei, each composed of two stacking

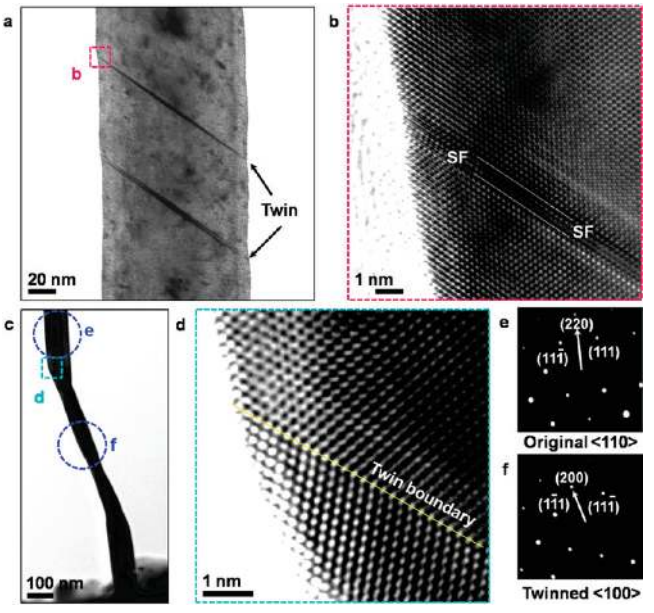

Figure 2. TEM images of a Au NW during the tensile deformation. (a) Two nanotwins initially nucleated in the plastic deformation. (b) HRTEM image magnified from the magenta square in (a). The twin is composed of two stacking faults (SFs), as clearly seen between two dotted lines in (b). (c) TEM micrograph showing a twin extended to 1 μm length by twin propagation (Supporting Information Figure S3). (d) HRTEM image magnified from the cyan square in (c), showing a clear twin boundary along the yellow line. (e,f) SAED patterns acquired from two blue dotted circles in (c) with a 180 nm aperture, the NW lattice is changed from an original ⟨110⟩ (e) to a twinned ⟨100⟩ (f).

faults generated by successive gliding of partial dislocations across the NW on neighboring {111} crystal planes at an initial stage of plastic deformation, corresponding to a stage between Figure 1 panels a and b. The initially nucleated twin is extended by the coherent twin propagation process to ∼1 μm length,

dx.doi.org/10.1021/nl2022306 |*Nano Lett.* 2011, 11, 3499–3502

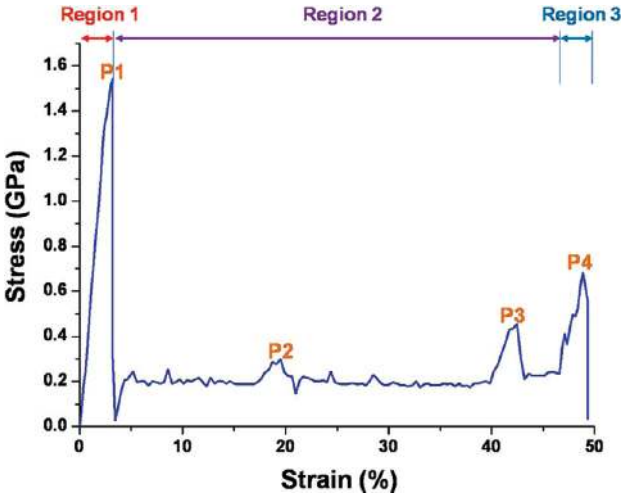

Figure 3. The stress−strain curve of a ⟨110⟩ Au NW for the whole tensile process. Region 1 represents elastic deformation, Region 2 represents the plastic deformation of a ⟨110⟩ Au NW, and Region 3 represents the deformation of a reoriented ⟨100⟩ Au NW.

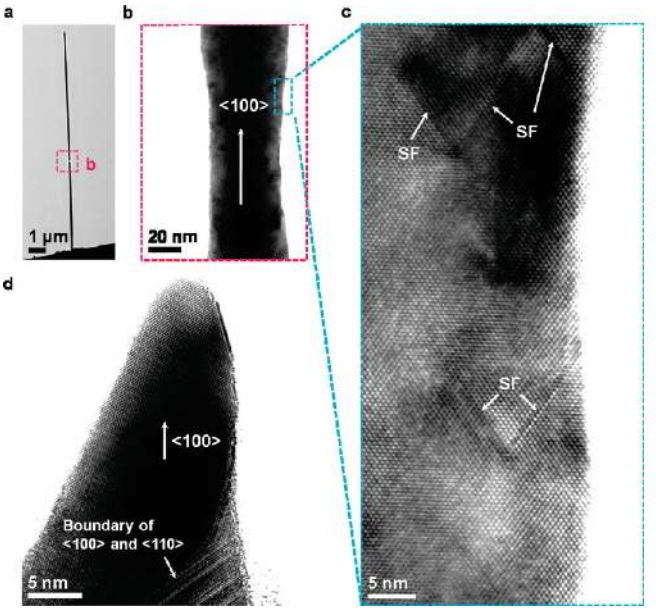

Figure 4. TEM images before and after fracture of a ⟨100⟩ Au NWs. (a−c) TEM images showing necking generated during the deformation of a single crystalline ⟨100⟩ NW, formed by the tensile stress-driven reorientation of a ⟨110⟩ Au NW. A TEM image (b) magnifies the magenta square in (a). (c) A magnified image of the cyan rectangle in (b), illustrating stacking faults (SFs) developed by the interactions of localized partial dislocations. (d) HRTEM image of a ⟨100⟩ NW fractured at the necked region (b), which is very close to the NW end.

showing a clear twin boundary (Figure 2d). TEM investigations revealed that the two initial twins seen in Figure 2a were combined to a single one by twin propagation. Selected area electron diffraction (SAED) patterns of the original and twinned regions (Figure 2e,f) show that the twin formation reorients the lattice of the NW from ⟨110⟩ to ⟨100⟩. The tensile deformation of fcc-structured metal NWs through twin propagation and accompanying lattice reorientation has been predicted by atomistic simulations.[11−13]

In addition to the atomic level observation of the tensile deformation by electron microscopes, we have successfully acquired the stress−strain curve of the tensile process of a Au NW from the load variation of a cantilever and the corresponding strain measured from SEM video images. Figure 3 illustrates the whole tensile process of the Au NW as displayed in Figure 1 in terms of stress−strain. The Au NW is not the same one as in Figure 1 and has diameters of 140.4 ± 0.5 and 101.2 ± 0.5 nm for the long axis and short axis, respectively. The tensile deformation can be described by three distinctive stages: superelastic and superstrong Region 1, superplastic Region 2, and Region 3 showing tensile process of a now-reoriented ⟨100⟩ NW. The stress−strain curve combined with electron microscope observation results provides a clear atomistic picture of the tensile deformation dynamics of a Au NW.

In Region 1, the deformation of a ⟨110⟩ NW begins with superelastic stretching up to 3.2% strain that ends with a high-yield strength of 1.54 GPa (Point 1) showing superstrength. The yield strength is significantly higher than the bulk value of Au, 55−200 MPa, and is close to a theoretical limit of 1.8 GPa.[17] We obtain 72 GPa for Young's modulus, as compared with 53−55 GPa of a bulk value and 78 GPa of a theoretical limit.[18,19] We interpret that the Au NWs become superstrong because they are defect-free and thus very close to the theoretically assumed perfect structure. Their nanosized diameters make them slightly less ideal than the theory,[20] leading to a lower yield strength and Young's modulus than the theoretical values.

The second stage (Region 2) starts with abrupt generation of nanotwins that decrease stress and continues with subsequent superplastic elongation by twin propagation. Note that the strain of 41% measured from the SEM images matches quite well with the geometric elongation ($\sqrt{2}$) expected from the lattice reorientation of a NW from ⟨110⟩ to ⟨100⟩. The stress−strain curve indicates that the flow stress required for the nucleation and propagation of a twin in a ⟨110⟩ Au NW is ∼200 MPa, much lower than the yield strength (1.54 GPa) for the first nucleation of a partial dislocation (point P1). Thus, the twin expansion is energetically much preferred to the nucleation of additional partial dislocations at other locations. Two small peaks (points P2 and P3) shown in the stress−strain curve can be attributed to the barriers imposed by other twins that were initially formed.

From the help of theoretical results,[12] we can explain the twin propagation mechanism as follows. At the yielding point (P1), a partial dislocation nucleates from one edge of the NW, glides across the NW on the {111} plane and promptly annihilates at the opposite edge. Second partial dislocation nucleates next to the first one, glides on the adjacent {111} plane and annihilates. By repeating this process, the twin propagates coherently along the NW axis to the end, inducing the observed superplasticity. The twin propagation converts the initial ⟨110⟩ NW having a rhombic cross section and {111} side facets to a ⟨100⟩ NW having a rectangular cross section and {100} side facets (Supporting Information Figure S4) through the deformation (Figure 2e and f).

The experimental stress−strain curve (Figure 3) has one-to-one correspondence with the snapshots and the in situ SEM movie that shows the whole tensile process (Figure 1 and Supporting Information Movie S1). Region 2 in Figure 3 corresponds to the twin propagation stage of Figure 1b−d, P1 in Figure 3 to Figure 1b representing a snapshot of initial twin growth stage right after the yielding, and Region 3 in Figure 3 to Figure 1e representing that of the tensile process of the reoriented ⟨100⟩ NW.

dx.doi.org/10.1021/nl2022306 |*Nano Lett.* 2011, 11, 3499–3502

After the tensile stress-driven reorientation of the Au NW from ⟨110⟩ to ⟨100⟩ was completed (Figure 1e), the final stage (Region 3) shows elastic deformation of a now ⟨100⟩ NW and its final fracture via necking by continued tensile loading. Geometric effect enforced by twin deformation induces necking in the ⟨100⟩ NW (Figure 4a−c) and finally leads to fracture at a rather low stress of ∼700 MPa (point P4) after a total strain of 2.8%. In order to eliminate the geometric effect, the ⟨100⟩ reorientated Au NW was cut by an FIB ion beam and realigned again. Its tensile measurements then show a yield strength of 1.1 GPa and Young's modulus of 35 GPa (Supporting Information Figure S5 and Movie 2).

The observed superstrength of a ⟨110⟩ Au NW is ascribed to the difficulty in initial dislocation nucleation at a perfectly crystalline Au NW.[20,21] On the other hand, the high aspect ratio of the Au NW as well as superb crystallinity is critical to the observed superplasticity. While superb crystallinity allows coherent extension of dislocations to a long distance, the nanometer-sized diameter of a Au NW induces prompt escape of the leading partial dislocations, thereby allowing progressive extension of a twin boundary by one lattice layer and ultimately leading to coherent propagation of the twin boundary to the end of a NW.

In conclusion, we have demonstrated through tensile deformation experiments that the defect-free Au NW shows superplasticity as well as superstrength. The unique mechanical properties of the Au NW are ascribed to its superb crystallinity and radial confinement. Large scale twin propagation of a Au NW observed here provides direct experimental evidence for predictions by atomistic simulations,[11−13] as well as deciphers central mechanical issues pursued by delicate experiments on tensile properties of NWs.[4,14−16,20] The ideal mechanical properties of the Au NWs would make them key elements in fabrication of novel nanomechanical devices, including highly reliable nanomedical devices. The distinct tensile properties of defect-free Au NWs could be observed in other fcc-structured metal NWs. If we can upscale this superstrong−superplastic material into a size of micrometers, it would contribute to critical improvement of conventional mechanical devices.

■ ASSOCIATED CONTENT

Supporting Information. Additional figures and movies with descriptions. This material is available free of charge via the Internet at http://pubs.acs.org.

■ AUTHOR INFORMATION

Corresponding Author

*E-mail: (J.-P.A.) jpahn@kist.re.kr; (B.K.) bongsoo@kaist.ac.kr.

Author Contributions

▽These authors contributed equally to this work.

■ ACKNOWLEDGMENT

J.-P.A. and B.K. acknowledge financial support by the KIST R&D program and by KOSEF through NRL (2011-0020419), SRC (2011-0001335), and CNMT (2011-K000210) of the MEST, Korea. We thank Prof. W. D. Nix and Dr. I. S. Choi for helpful discussions.

■ REFERENCES

(1) Uchic, M. D.; Dimiduk, D. M.; Florando, J. N.; Nix, W. D. *Science* **2004**, *305*, 986.
(2) Lu, L.; Chen, X.; Huang, X.; Lu, K. *Science* **2009**, *323*, 607.
(3) Wang, Y.; Chen, M.; Zhou, F.; Ma, E. *Nature* **2002**, *419*, 912.
(4) Wu, B.; Heidelberg, A.; Boland, J. J. *Nat. Mater.* **2005**, *4*, 525.
(5) Rupert, T. J.; Gianola, D. S.; Gan, Y.; Hemker, K. J. *Science* **2009**, *326*, 1686.
(6) Yu, Q.; Shan, Z.-W.; Li, J.; Huang, X.; Xiao, L.; Sun, J.; Ma, E. *Nature* **2010**, *463*, 335.
(7) Chen, K. C.; Wu, W. W.; Liao, C. N.; Chen, L. J.; Tu, K. N. *Science* **2008**, *321*, 1066.
(8) Oh, S. H.; Legros, M.; Kiener, D.; Dehm, G. *Nat. Mater.* **2009**, *8*, 95.
(9) Narayan, J. *J. Appl. Phys.* **2006**, *100*, 034309.
(10) Yoo, Y.; Seo, K.; Han, S.; Varadwaj, K.; Kim, H.; Ryu, J.; Lee, H.; Ahn, J.; Ihee, H.; Kim, B. *Nano Lett.* **2010**, *10*, 432.
(11) Park, H. S.; Gall, K.; Zimmerman, J. A. *Phys. Rev. Lett.* **2005**, *95*, 255504.
(12) Liang, W.; Zhou, M.; Ke, F. *Nano Lett.* **2005**, *5*, 2039.
(13) Leach, A. M.; McDowell, M.; Gall, K. *Adv. Funct. Mater.* **2007**, *17*, 43.
(14) Richter, G.; Hillerich, K.; Gianola, D. S.; Mönig, R.; Kraft, O.; Volkert, C. A. *Nano Lett.* **2009**, *9*, 3048.
(15) Zhu, Y.; Xu, F.; Qin, Q.; Fung, Y.; Ku, W. *Nano Lett.* **2009**, *9*, 3934.
(16) Han, X. D.; Zheng, K.; Zhang, Y. F.; Zhang, X. N.; Zhang, Z.; Wang, Z. L. *Adv. Mater.* **2007**, *19*, 2112.
(17) Ogata, S.; Li, J.; Hirosaki, N.; Shibutani, Y.; Yip, S. *Phys. Rev. B* **2004**, *70*, 104104.
(18) Espinosa, H. D.; Prorok, B. C.; Peng, B. *J. Mech. Phys. Solids* **2004**, *52*, 667.
(19) Callister, W. D. *Materials science and engineering*; Wiley: New York, 1994; Chapters 6−8.
(20) Zhu, T.; Li, J.; Samanta, A.; Leach, A.; Gall, K. *Phys. Rev. Lett.* **2008**, *100*, 025502.
(21) Zheng, H.; Cao, A.; Weinberger, C. R.; Huang, J. Y.; Du, K.; Wang, J.; Ma, Y.; Xia, Y.; Mao, S. X. *Nat. Commun.* **2010**, *1*, 144.